RSC Advances

ROYAL SOCIETY OF CHEMISTRY

www.rsc.org/advances

A novel aptamer-mediated $CuInS_2$ quantum dots@graphene oxide nanocomposites-based fluorescence "turn off-on" nanosensor for highly sensitive and selective detection of kanamycin

Ziping Liu[a], Chengshuo Tian[a], Lehui Lu [b] and Xingguang Su[a*]

[a] *Department of Analytical Chemistry, College of Chemistry, Jilin University, Changchun 130012, P.R. China*

[b] *State Key Laboratory of Electroanalytical Chemistry, Changchun Institute of Applied Chemistry, Chinese Academy of Sciences, Changchun, 130022, China*

*Corresponding author

Tel.: +86-431-85168352

E-mail address: suxg@jlu.edu.cn

Abstract

In this paper, we designed a novel near-infrared aptamer-mediated fluorescence "turn off-on" nanosensor for highly sensitive and selective detection of kanamycin based on $CuInS_2$ quantum dots (QDs)@graphene oxide (GO) nanocomposites. The carboxy groups on the surface of $CuInS_2$ QDs (modified with mercaptopropionic acid) were conjugated with amino terminal kanamycin-binding Ky2 aptamer to form the Ky2-$CuInS_2$ QDs in the presence of 1-(3-dimethylaminopropyl)-3-ethylcarbodiimide hydrochloride and *N*-hydroxysuccinimide. Then, the Ky2-$CuInS_2$ QDs were facilely immobilized on the surface of GO through π-π stacking interaction between the nucleobases and GO, which caused the fluorescence of Ky2-$CuInS_2$ QDs "turned off". In the presence of kanamycin, the Ky2-$CuInS_2$ QDs desorb from the surface of GO and bind to kanamycin with high affinity and specificity. As a result, the quenched fluorescence "turned on". Under the optimum conditions, there was a good linear relationship between I/I_0 (I and I_0 were the fluorescence intensity of Ky2-$CuInS_2$ QDs@GO in the presence and absence of kanamycin, respectively) and kanamycin concentration in the range of 0.3-45 $nmol \cdot L^{-1}$ (0.174-26.1 $\mu g \cdot L^{-1}$), with the detection limit of 0.12 $nmol \cdot L^{-1}$ (0.070 $\mu g \cdot L^{-1}$). The present nanosensor was utilized to detect kanamycin in the human serum, urine and milk samples with satisfactory results.

1. Introduction

Kanamycin is an important aminoglycoside antibiotic that can inhibit the biosynthesis of protein through binding to the 30S subunit of ribosomal, which ultimately misreads the genetic code and disturbs the translation.[1] It is widely used as a broad-spectrum antibiotic in veterinary medicine and as a second-line antibiotic in the treatment of serious infections caused by various pathogenic bacteria.[2] However, kanamycin exhibits comparatively narrow safety margin similar to the other antibiotics. Kanamycin overdose is capable of producing some rather serious adverse effects, such as loss of hearing, toxicity to kidneys, and allergic reactions to the drugs.[3] Considering the potential transfer and accumulation effect of kanamycin in human bodies in the food chain, many countries have begun to monitor the residual kanamycin in foodstuffs nowadays. European Union (EU) has mandated the maximum residue limits (MRLs) for kanamycin in milk and edible tissues: 150 $\mu g \cdot kg^{-1}$ in milk (approximately equal to 300 nM), 100 $\mu g \cdot kg^{-1}$ for meat, 600 $\mu g \cdot kg^{-1}$ for liver and 2500 $\mu g \cdot kg^{-1}$ for kidney.[4]

So far, there are many assays for kanamycin quantification and/or detection. The traditional methods, which were commonly used, were high performance liquid chromatography (HPLC)[5] and enzyme-linked immunosorbent assay (ELISA).[6] Although HPLC methods are indispensable in terms of confirmation, they require expensive instrumentation, highly skilled personnel and complex sample preparation steps. ELISAs could offer quantitive detection with high specificity. However, they would become time-consuming and laborious when a large number of samples must

be screened. Besides, the involvement of radioisotope labels and specific antibodies among ELISAs may lead to a potential security risk and narrow application scope. In the recent years, some other strategies have been exploited for kanamycin detection, such as capillary electrophoresis (CE),[7] electrochemical immunosensor (EI)[8] and surface plasmon resonance (SPR).[9] For electrochemical strategies, the complicated electrode modification processes are generally laborious and time-consuming, which are not suitable for routine analysis of a large number of samples. Most of the SPR-based sensors developed nowdays were targeting one compound or a family of structurally or functionally similar compounds, resulting in assays with a rather narrow detection spectrum.

Fluorescence strategies are an attractive alternative for the determination of kanamycin because of their safety, simplicity, speediness, high sensitivity and most importantly, amenability to high-throughput screening.[10] Especially in recent years, with the rapid development of nanotechnology, various fluorescence nanomaterials have been utilized to develop optical nanosensors, such as carbon nanotubes,[11] metal oxides[12] and metal nanoparticles.[13] Among them, semiconductor quantum dots (QDs) have attracted considerable attention due to their unique electro-optical properties, including high quantum yields, large extinction coefficients, long fluorescence lifetimes, pronounced photostability, and broad absorption spectra coupled with narrow photoluminescent emission spectra.[14] However, the applications of QDs are hampered owing to the high toxicity of the QDs and eventually would cause serious environmental problems.[15] Recently, as a novel class of toxic heavy metalfree

emitters that do not contain any toxic class A elements (Cd, Pb, and Hg) or class B elements (Se and As), the newly developed water-soluble I-III-VI $CuInS_2$ QDs have attracted increasing research interests.[16]

Graphene oxide (GO), which is rich of oxygen-containing groups (*e.g.* carboxyl, epoxy hydroxyl groups) on its surface, has received enormous attention because of its versatility including extremely hydrophilic, unique DNA adsorbing ability and excellent electronic and photophysical features.[17] Moreover, GO has proven to be an efficient fluorescence quencher, which plays a major role in its biological application, such as nucleic acids assays,[18] proteins assays,[19] enzyme activity detections[20] and other small molecules.[21] Since Yang's group reported a graphene sensing platform for biomolecules, which based on förster resonance energy transfer (FRET) between fluorescent dye and graphene oxide through strong adsorption of labeled DNA on graphene oxide,[22] a variety of GO-based fluorescence sensors have been developed.

Aptamer are single stranded oligonucleotides with specific sequences (DNA or RNA molecules), they are capable of recognizing and binding to their cognate targets (ranging from small molecules to heavy metals, proteins, cells and even intact viral particles) with high affinity and specificity.[23] Due to their unique advantages including low cost and easy in vitro synthesis and chemical modification, less immunogenic response, high chemical stability, and inherent binding affinity, a range of aptamer-based biosensing platforms have been developed.[24]

Herein, we report a novel fluorescence "turn off-on" nanosensor for specific detection of kanamycin using low-cost, unmodified and label-free DNA aptamer in

cooperation with water-dispersible GO and $CuInS_2$ QDs nanocomposites. Firstly, mercaptopropionic acid modified $CuInS_2$ QDs were directly prepared in aqueous solution via a hydrothermal synthesis method. Then, the carboxy groups on the surface of $CuInS_2$ QDs were conjugated with amino terminal kanamycin-binding DNA aptamer Ky2 (5'-TGGGGGTTGA GGCTAAGCCGA-3') in the presence of 1-(3-dimethylaminopropyl)-3-ethylcarbodiimide hydrochloride (EDC) and *N*-hydroxysuccinimide (NHS), forming the aptamer functionalized $CuInS_2$ QDs (Ky2-$CuInS_2$ QDs). Because of the large specific surface area and π-conjugated structure of GO, the kanamycin aptamer Ky2 could be facilely immobilized on the surface of GO through π-π stacking interaction between the nucleobases and GO, causing the fluorescence of Ky2-$CuInS_2$ QDs "turned off" via förster resonance energy transfer (FRET) process. [25,26] While kanamycin molecules were present in the solution, the Ky2-$CuInS_2$ QDs could specifically and sensitively bind kanamycin molecules[27] and actived the fluorescence to a "turn on" state.

2. Experimental

2.1. Materials and Instruments

All chemicals and reagents were of at least analytical reagent grade and used directly without any further purification. Copper (II) chloride dehydrate ($CuCl_2 \cdot 2H_2O$), sulfourea ($CS(NH_2)_2$), indium (III) chloride tetrahydrate ($InCl_3 \cdot 4H_2O$), mercaptopropionic acid (MPA) and kanamycin were purchased from Sigma-Aldrich Corporation. 1-ethyl-3-[3-dimethylaminopropyl] carbodiimide hydrochloride (EDC)

was purchased from Beijing Chemical Works. Kanamycin, sodium hydroxide (NaOH), streptomycin, chloramphenicol, erythromycin, sulfadimethoxine, chlorotetracycline and the other chemicals used were all purchased from Beijing Dingguo Changsheng Biotechnology Co. Ltd. The sequence for kanamycin aptamer Ky2 [5'-TGGGGGTTGAGGCTAAGCCGA-3'] was synthesized by Shanghai Sangon Biotechnology Co. Ltd. The water used in all experiments had a resistivity higher than 18 $M\Omega \cdot cm^{-1}$.

Fluorescence measurements were performed on a Shimadzu RF-5301 PC spectrofluorophotometer (Shimadzu Co., Kyoto, Japan) and a 1 cm path-length quartz cuvette was used in all experiments. UV-vis absorption spectra were obtained using a Varian GBC Cintra 10e UV-vis spectrometer. All pH measurements were taken with a PHS-3C pH meter (Tuopu Co., Hangzhou, China).

2.2. Synthesis of MPA-capped $CuInS_2$ QDs

$CuInS_2$ QDs (capped by mercaptopropionic acid) were prepared in aqueous solution via a hydrothermal synthesis method according to our previous report.[28] In a typical experiment, $InCl_3 \cdot 4H_2O$ (0.15 mmol) and $CuCl_2 \cdot 2H_2O$ (0.15 mmol) were dissolved in 7.5 mL distilled water, and then mercaptopropionic acid (1.80 mmol) was injected into the solution. The pH value of the mixture solution was adjusted to 11.3 by adding 4 $mol \cdot L^{-1}$ NaOH solution with stirring. After stirring for 10 min, $CS(NH_2)_2$ (0.30 mmol) was dissolved in the solution. The Cu-to-In-to-S and Cu-to-mercaptopropionic acid precursor ratios were 1:1:2 and 1:12, respectively. All the above mentioned experimental procedures were performed at room temperature, and then the solution

was transferred into a Teflon-lined stainless steel autoclave with a volume of 15 mL. The autoclave was maintained at 150℃ for 23 h and then cooled down to room temperature by a hydro-cooling process. The final concentration of $CuInS_2$ QDs, as measured by the In^{3+} concentration, was 1.36×10^{-4} mol·L^{-1}.

2.3. Conjugation of Ky2 aptamers with $CuInS_2$ QDs

Firstly, the mercaptopropionic acid modified $CuInS_2$ QDs was activated for 30 min in the presence of EDC and NHS (the mole ratio of QDs to EDC to NHS was 1:1500:1500). The resulting N-hydroxy-succinimide-activated $CuInS_2$ QDs solutions were then mixed with to amine modified kanamycin aptamer (the mole ratio of aptamer to QDs was 1:544). The mixture was incubated at room temperature with gentle shaking for 3 h. The unreacted kanamycin aptamer were removed by dialysis against phosphate buffered saline in a dialysis membrane. All the buffer solution used in the experiment was at a pH 7.4 PBS (10 mmol·L^{-1}) containing 10 mmol·L^{-1} NaCl.

2.4. Synthesis of graphene oxide

Graphene oxide (GO) was synthesized according to modified Hummer's method which was mentioned and characterized in our previous work.[29] Briefly, the graphite powder (2 g) was dispersed in concentrated H_2SO_4 (44 mL) and incubated for 15 min under the condition of ice-water bath. $KMnO_4$ (6 g) was then added gradually into the solution under stirring with the temperature below 20 ℃. This mixture was stirred at 15 ℃ for 20 min and reacted at 35 ℃ for 1 h. Subsequently, deionized water (160 mL) was dropwise added to dilute the mixture. After the resulting mixture was kept at 60 ℃ for 15 min, water (200 mL) and 30% H_2O_2 (20 mL) were added to end the

reaction. The mixture was washed with deionized water to remove the acid. Then, the product was further purified by dialysis for 1 week to remove the remaining metal species. Exfoliation was carried out by sonicating graphite oxide under ambient conditions for 30 min. The obtained dispersion was centrifuged at 5000 rpm to remove any unexfoliated graphene oxide. The resultant graphene oxide (1.88 mg·mL^{-1}) was stored at room temperature and employed in the following experiments.

2.5. Fluorescence experiments

In fluorescence experiments, pH 7.4 PBS (Phosphate Buffered Saline, 10 mmol·L^{-1}) containing 15 mmol·L^{-1} NaCl was used for dilution. A series of 200 μL Ky2-$CuInS_2$ QDs solutions (the mole ratio of aptamer to QDs was 1:544) were placed in a series of 2.0 mL calibrated test tubes. Subsequently, 10 μL GO was then added into the above solution, respectively. The mixtures were incubated 20 min at the room temperature, and then different amounts of kanamycin were added and mixed thoroughly, respectively. 40 min later, the fluorescence spectra were recorded in the 610-800 nm emission wavelength range at an excitation wavelength of 590 nm.

2.6. Samples assay

The liquid dairy milk was bought from a local supermarket. Some necessary processes were conducted to remove impurities to get the milk samples before carrying out fluorescence experiments. Firstly, the milk samples were filtered through a 0.22 μm membrane. Then, liquid milk (1 mL), acetonitrile (1.5 mL) and 10% trichloroacetic acid (7.5 mL) were mixed in a centrifuge tube and centrifuged at 10,000 rpm for 5 min to precipitate protein and dissolve organic substances. Subsequently, the middle

liquid layer was spiked with different kanamycin solutions to final concentrations at three levels (0.5, 1.0 and 1.5 nM). Detection processes were carried out according to the above mentioned optimized conditions for kanamycin detection.

The fresh human blood samples were collected from healthy volunteer through venipuncture at the Hospital of Changchun China, Japan Union Hospital. All experiments were performed in compliance with the relevant laws and institutional guidelines, and the writing of informed consent for all samples was obtained from human subjects. Before carrying out fluorescence experiments, the blood samples were segregated by adding acetonitrile (the volume of acetonitrile and blood was 1.5: 1) and centrifuged at 10,000 rpm for 5 min after stored for 2 h at room temperature. Then, all supernatant serum samples were subjected to a 100-fold dilution with PBS before analysis, and a certain concentration of kanamycin was added to prepare the spiked samples. These samples were detected with the fluorescence measurements under the optimal conditions. The human urine samples obtained from healthy volunteers were collected. The urine samples were diluted 10 times with PBS before detection.

3. Results and discussion

3.1. The strategy for the detection of kanamycin

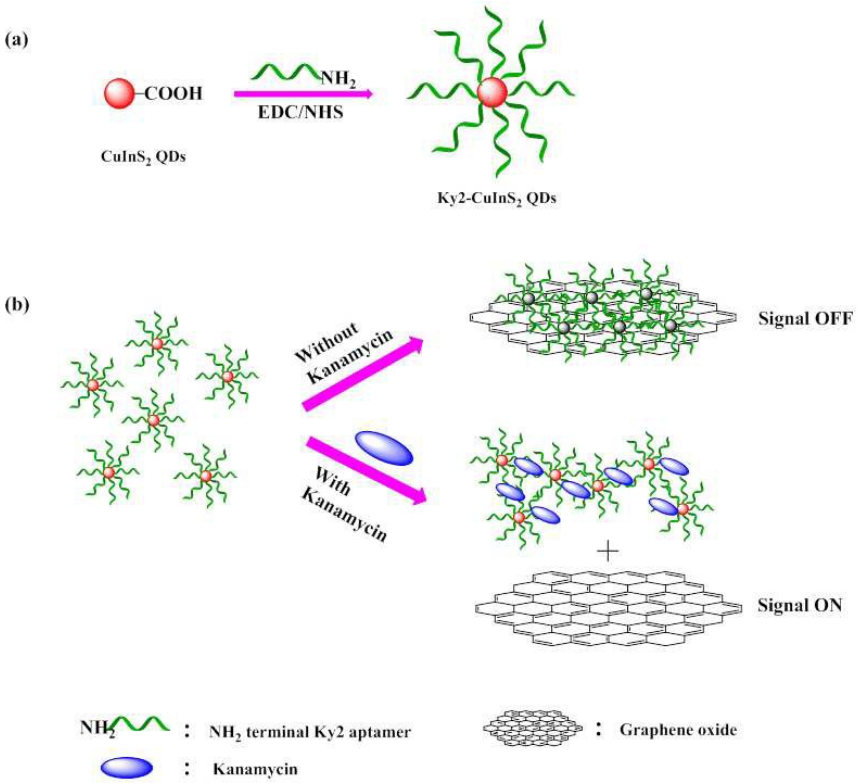

Scheme 1 Schematic illustration for fabrication of Ky2-$CuInS_2$ QDs (a); Schematic representation of the novel fluorescence "turn off-on" bionanosensor for kanamycin detection based on Ky2-$CuInS_2$ QDs and graphene oxide (b).

As illustrated in Scheme 1 (a), mercaptopropionic acid modified $CuInS_2$ QDs were covalently linked to NH_2 terminal Ky 2 aptamer in the presence of EDC and NHS to form Ky2-$CuInS_2$ QDs. Fig. 1 (a) was the TEM image of the as-prepared $CuInS_2$ QDs. From Fig. 1 (a), it can be seen that the as-prepared $CuInS_2$ QDs were spherical particles with good monodispersity, and the average size was 3.23 nm (with a standard deviation of 2.79%). Fig. 1 (b) was the DLS of the MPA-capped $CuInS_2$ QDs. From Fig. 1 (b), it could be seen that the generated $CuInS_2$ QDs are nearly monodispersed with the diameter from 1 nm to 5 nm, and an average diameter of 3.20 nm (with a standard deviation of 1.12%). The luminescence quantum yield of the

ternary QDs used in this work was 3.4%, which was higher than that synthesized in organic solvent (QY=3%).[30] Fig. S1 was the fluorescence decay curves of $CuInS_2$ QDs in aqueous solution. The decay curves can be fitted to a biexponential model, and the average fluorescence lifetime of $CuInS_2$ QDs was 181.7 ns, which is in accordance with previous report.[31] Fig. 1 (c) was zeta potential of MPA-$CuInS_2$ QDs (black column) and Ky2-$CuInS_2$ QDs (red column). Based on previous reports, solutions with zeta potential above +20 mV and below -20 mV are considered stable.[32] The zeta potential of MPA-$CuInS_2$ QDs was -37.90 mV, which indicated that the generated MPA-$CuInS_2$ QDs are stable in the solution. After the attachment of the Ky2 aptamer onto $CuInS_2$ QDs, the zeta potential of Ky2-$CuInS_2$ QDs was -46.17 mV, which might be result from the negative charge of Ky2 aptamer. Fig. 1 (d) was the UV-vis absorption spectra of $CuInS_2$ QDs, Ky2 aptamer and Ky2-$CuInS_2$ QDs and Fig. 1 (e) was the corresponding fluorescence emission spectra of $CuInS_2$ QDs and Ky2-$CuInS_2$ QDs. It could be observed that $CuInS_2$ QDs showed the major absorption band at around 580 nm.[33] And Ky2 aptamer exhibited its typical absorption spectrum at around 240 nm.[34] Compared with the respective absorption spectrum of $CuInS_2$ QDs and Ky2-$CuInS_2$ QDs, both absorption peaks at around 240 nm and 580 nm was observed in the absorption spectra of Ky2-$CuInS_2$ QDs, which demonstrated the successful conjugation of the exterior free carboxyl of $CuInS_2$ QDs and the NH_2 terminal Ky2 aptamer. The slightly enhanced of the corresponding fluorescence emission spectra of Ky2-$CuInS_2$ QDs further confirmed that the successful conjugation. Surface modification of QDs often changed their physicochemical

properties. [35,36] It was supposed that the slightly fluorescence enhancement was caused by the change of the surface functional group, and increased the resistance of QDs against oxidation to some extent.

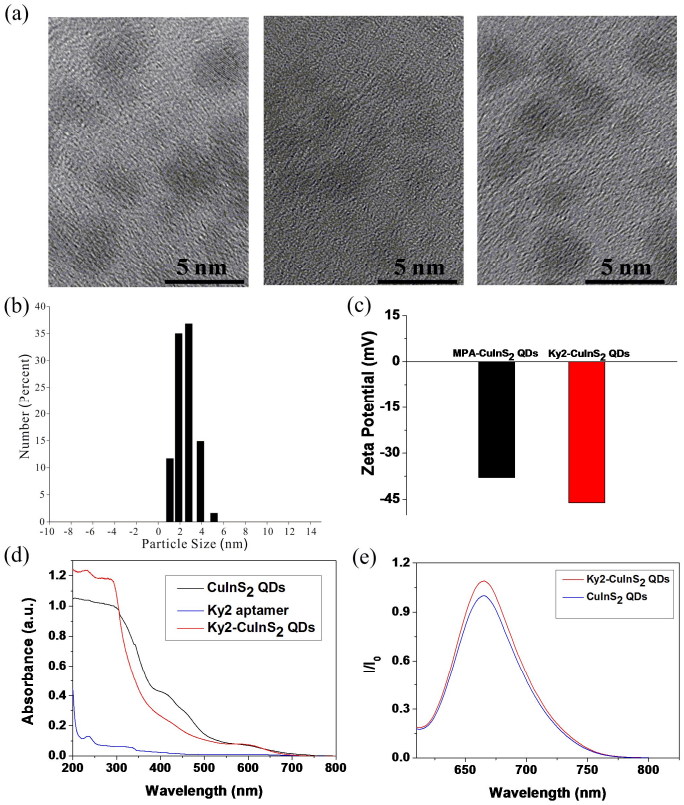

Fig. 1 (a) The TEM image of the as-prepared $CuInS_2$ QDs; (b) Dynamic light scattering data of MPA capped $CuInS_2$ QDs; (c) Zeta potentials of MPA capped-$CuInS_2$ QDs (black column) and Ky2-$CuInS_2$ QDs (red column); (d) UV-vis spectra of $CuInS_2$ QDs, Ky2 aptamer and Ky2-$CuInS_2$ QDs; (e) The corresponding fluorescence emission spectra of $CuInS_2$ QDs and Ky2-$CuInS_2$ QDs. The excitation wavelength was 590 nm.

The FT-IR spectra of the MPA capped $CuInS_2$ QDs and Ky2-$CuInS_2$ QDs were shown in Fig. S2 to further demonstrate the formation of Ky2-$CuInS_2$ QDs. In Fig. S2 (green curve), the majority of MPA functional groups could be clearly found through the characteristic peaks of -COOH (1560 cm^{-1} asymmetric stretching vibration, 1470

cm^{-1} symmetric stretching vibration), and and -CH_2 (2859 cm^{-1} symmetric stretching vibration). We could ascertain that the original $CuInS_2$ QDs were capped by MPA. For Ky2-$CuInS_2$ QDs, as shown in Fig. S2 (red curve), peaks assigned to -COOH decreased, while the peaks for the asymmetric stretching vibrations of the PO_2^- (1280 cm^{-1}), and the P-O stretches of the main chain (930 cm^{-1}) appeared. These results indicated that the Ky2 aptamer were successfully linked to the surface of the $CuInS_2$ QDs.

The illustration in Scheme 1 (b) represented the principle of the fluorescence "turn off-on" nanosensor for kanamycin detection based on Ky2-$CuInS_2$ QDs and GO. The large specific surface area and π-π conjugated structure of GO could provide an excellent platform for immobilizing the kanamycin binding aptamer on the surface via π-π stacking interaction. In addition, GO had a higher quenching efficiency, which was beneficial to the construction a fluorescence "turn off-on" mode sensor with low background, high signal to noise ratio and ultrasensitivity. In the absence of kanamycin, Ky2-$CuInS_2$ QDs would absorb onto the GO surface via π-π stacking interaction and the intrinsic strong fluorescence intensity of Ky2-$CuInS_2$ QDs was quenched through FRET process (Ky2-$CuInS_2$ QDs as donor and GO as acceptor). While in the presence of kanamycin, Ky2-$CuInS_2$ QDs would selectively bind with kanamycin with high affinity to form Ky2-$CuInS_2$ QDs/kanamycin complex, which could block the FRET process between Ky2-$CuInS_2$ QDs and GO, thus the fluorescence of Ky2-$CuInS_2$ QDs become "turn on". The fluorescence emission spectra of Ky2-$CuInS_2$ QDs, Ky2-$CuInS_2$ QDs/GO and Ky2-$CuInS_2$

QDs/GO/kanamycin were shown in Fig. 2. From Fig. 2, it can be seen that Ky2-$CuInS_2$ QDs had a narrow and symmetrica fluorescence spectrum with a maximum peak around 665 nm. After the addition of GO, the fluorescence intensity of Ky2-$CuInS_2$ QDs dramatically decreased, and 18.80 mg·mL^{-1} GO presented a quenching effect of ~90%. In the presence of kanamycin, the quenched fluorescence was recovered and 45 nmol·L^{-1} kanamycin presented a restoring effect of ~66%.

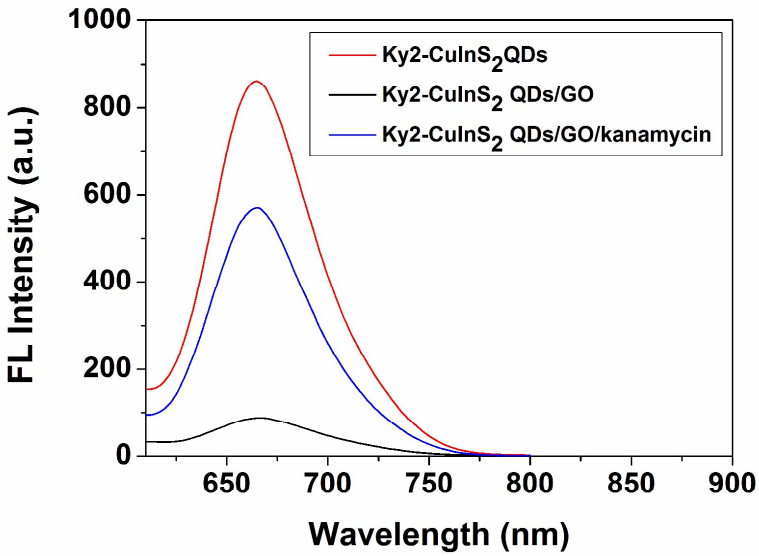

Fig. 2 The fluorescence emission spectra of Ky2-$CuInS_2$ QDs, Ky2-$CuInS_2$ QDs/GO and Ky2-$CuInS_2$ QDs/GO/kanamycin. The mole ratio of aptamer to QDs was 1:544. The concentration of GO was 18.80 μg·mL^{-1}. The excitation wavelength was 590 nm.

3.2. Optimization of the sensing procedure

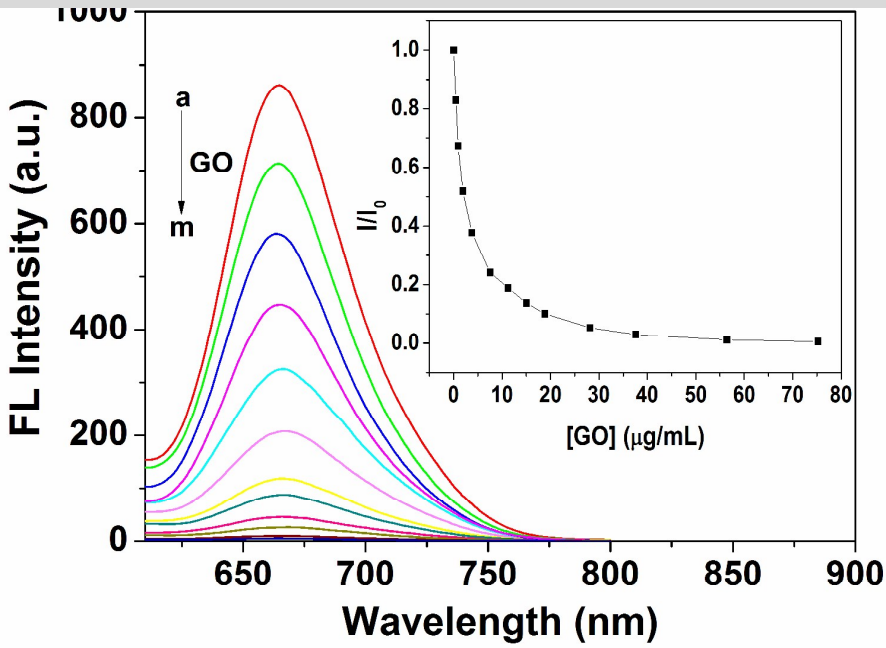

Fig. 3 The fluorescence spectra of Ky2-$CuInS_2$ QDs in the presence of different concentrations of GO. a-m represented the concentrations of GO of 0, 0.47, 0.94, 1.88, 3.76, 7.52, 11.28, 15.04, 18.80, 28.20, 37.60, 56.40 and 75.20 μg·mL^{-1}, respectively. Inset: The relationship between I/I_0 and the concentration of GO (from 0 to 75.20 μg·mL^{-1}). I and I_0 were the fluorescence intensity of Ky2-$CuInS_2$ QDs in the presence and absence of GO, respectively. The mole ratio of aptamer to QDs was 1:544. The excitation wavelength was 590 nm.

Firstly, we studied the quenching effect of GO on the fluorescence of Ky2-$CuInS_2$ QDs. From Fig. 3, it can be seen that the fluorescence intensity of Ky2-$CuInS_2$ QDs at 665 nm had a sharply decrease with the increasing concentration of GO in the range of 0-18.80 μg·mL^{-1}. Then the downward trend flattened out and a plain appeared in the concentration range of 28.20-75.20 μg·mL^{-1}. The inset in Fig. 3 showed the relationship between the fluorescence intensity ratio I/I_0 and the concentration of GO (from 0 to 75.20 μg·mL^{-1}). I and I_0 were the fluorescence intensity of Ky2-$CuInS_2$

QDs in the presence and absence of GO, respectively. From the inset in Fig. 3, it can be seen that GO (18.80 μg·mL^{-1}) presented a quenching effect of ~90%. A GO concentration of 18.80 μg·mL^{-1} was choosen in the further experiments. As shown in Fig. S3, the relationship between the quenched fluorescence intensity of Ky2-$CuInS_2$ QDs and the concentration of GO could be described by a Stern-Volmer equation:

$$I_0/I=1.0610+0.4149[GO],\ \mu g\cdot mL^{-1}$$

It can be seen that Stern-Volmer constant K_{SV} is 0.4149 μg·mL^{-1}.

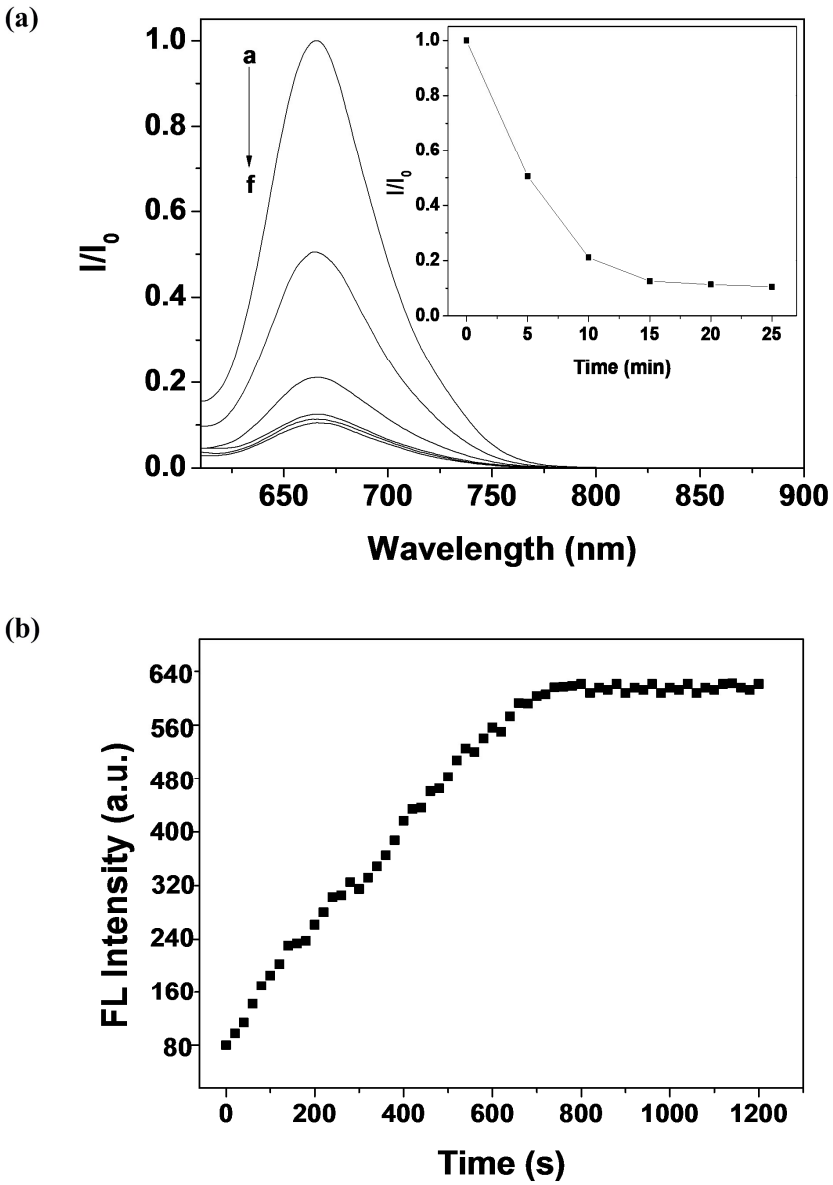

Fig. 4 (a) The quenching effect of GO on the fluorescence intensity of Ky2-$CuInS_2$ QDs in different incubation time. a-f represented the incubation time (0, 5, 10, 15, 20 and 25 min, respectively). Inset: The relationship between I/I_0 and the incubation time. I and I_0 were the fluorescence intensity of Ky2-$CuInS_2$ QDs in the presence and absence of GO, respectively. (b) The effect of restored time on the fluorescence intensity of the Ky2-$CuInS_2$ QDs/GO/kanamycin system. The mole ratio of aptamer to QDs was 1:544. The concentration of GO and kanamycin was 18.80 $\mu g \cdot mL^{-1}$ and 45 $nmol \cdot L^{-1}$. The excitation wavelength was 590 nm.

Then, we studied the quenching effect of GO on the fluorescence intensity of Ky2-$CuInS_2$ QDs in the different incubation time. The results in Fig. 4 (a) showed that the fluorescence intensity decreased sharply in the first 10 min of incubation time, and then decreased gradually with the increasing of incubation time until 15 min. Therefore, the fluorescence intensity was recorded after 15 min in the further experiments. The effect of restored time of the fluorescence intensity of the Ky2-$CuInS_2$ QDs/GO/kanamycin system was investigated. The results in Fig. 4 (b) showed that the FL intensity of the Ky2-$CuInS_2$ QDs/GO/kanamycin system significantly enhanced in the first 10 min and reached a balance at about 12 min. Thus, 15 min was chosed as the adequate reaction time for the further experiments.

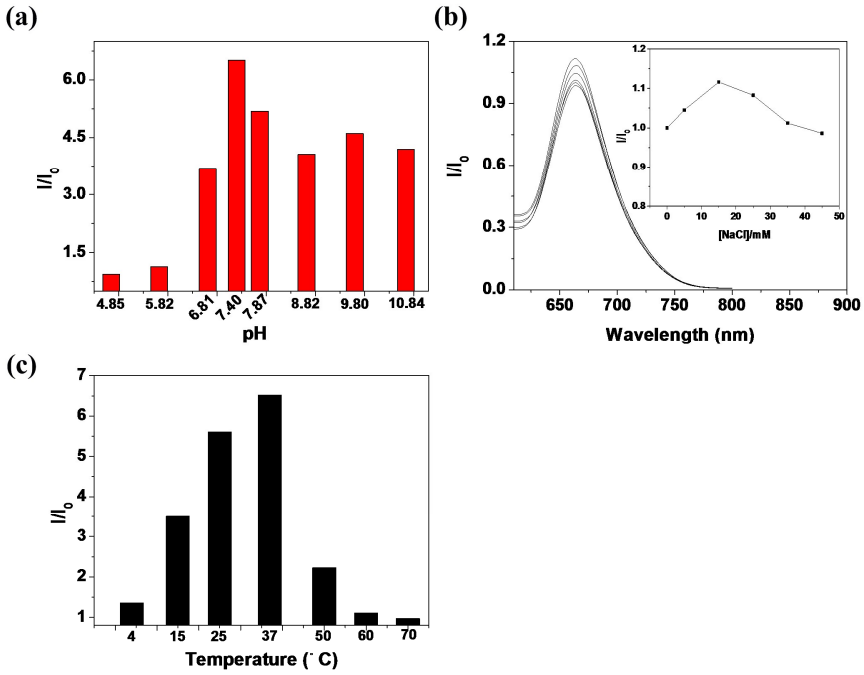

Fig. 5 (a) The effect of pH (4.85, 5.82, 6.81, 7.40, 7.87, 8.82, 9.80 and 10.84, respectively) on the fluorescence

intensity of Ky2-$CuInS_2$ QDs/GO/kanamycin system. I and I_0 were the fluorescence intensity of Ky2-$CuInS_2$ QDs/GO with and without of kanamycin, respectively. (b) The effect of salt concentration on the fluorescence intensity of Ky2-$CuInS_2$ QDs/GO/kanamycin system. Inset: The relationship between I/I_0 and different concentrations of NaCl. I and I_0 were the fluorescence intensity of Ky2-$CuInS_2$ QDs/GO/kanamycin with and without of NaCl, respectively. (c) The effect of temperature (4 ℃, 15 ℃, 25 ℃, 37 ℃, 50 ℃, 60 ℃ and 70 ℃, respectively) on the fluorescence intensity of Ky2-$CuInS_2$ QDs/GO/kanamycin system. I and I_0 were the fluorescence intensity of Ky2-$CuInS_2$ QDs/GO with and without of kanamycin, respectively. The mole ratio of aptamer to QDs was 1:544. The concentration of GO was 18.80 $mg \cdot mL^{-1}$. The concentration of GO and kanamycin was 18.80 $\mu g \cdot mL^{-1}$ and 45 $nmol \cdot L^{-1}$. The excitation wavelength was 590 nm.

For better sensing performance, we further optimized the experiment conditions including pH, salt concentration and incubation temperature. Fig. 5 (a) shows the effect of pH on the fluorescence intensity of Ky2-$CuInS_2$ QDs/GO/kanamycin system. I and I_0 were the fluorescence intensity of Ky2-$CuInS_2$ QDs/GO system in the presence and absence of kanamycin, respectively. From Fig. 5 (a), it can be found that the fluorescence intensity ratio (I/I_0) was much lower in acidic medium. This may be attributed to the protonation of the thymine bases of the kanamycin aptamer under acidic conditions, which could possibly result in a low binding affinity towards kanamycin.[37] The maximum value of I/I_0 appeared at the pH value of 7.40. When in alkaline medium, the fluorescence intensity ratio (I/I_0) became decreased. This may be resulted from possible base-catalysed hydrolysis of kanamycin at higher pH values.[32] Thus, all subsequent experiments were performed in 0.01 M PBS of pH 7.40. Fig. 5 (b)

was the effect of salt concentration on the fluorescence intensity of Ky2-$CuInS_2$ QDs/GO/kanamycin system. The inset of Fig. 5 (b) showed the relationship between I/I_0 and the concentrations of NaCl. I and I_0 were the fluorescence intensity of Ky2-$CuInS_2$ QDs/GO/kanamycin in the presence and absence of NaCl. The results in Fig. 5 (b) revealed that the ionic strength had no significant effect on the FL intensity of Ky2-$CuInS_2$ QDs/GO/kanamycin system. A NaCl concentration of 15 $mmol \cdot L^{-1}$ was selected in the subsequent experiments. Fig. 5 (c) was the influence of incubation temperature (ranging from 4 to 70 ℃) on the fluorescence intensity of Ky2-$CuInS_2$ QDs/GO/kanamycin system. I and I_0 were the fluorescence intensity of Ky2-$CuInS_2$ QDs/GO in the presence and absence of kanamycin, respectively. It can be observed that I/I_0 increased significantly with the increasing temperature from 4 to 37℃ and then decreased rapidly≥37℃. Fig. S4 was the secondary structure of the Ky2 aptamer predicted by M-Fold tool based on Zuker algorithm.[38] According to the previous report, the aptamer structure would be partial denaturalized at the elevated temperatures, and as a result the I/I_0 decreased.[39] Finally, 37℃ was selected as the optimal temperature.

3.3. Fluorescence detection of kanamycin

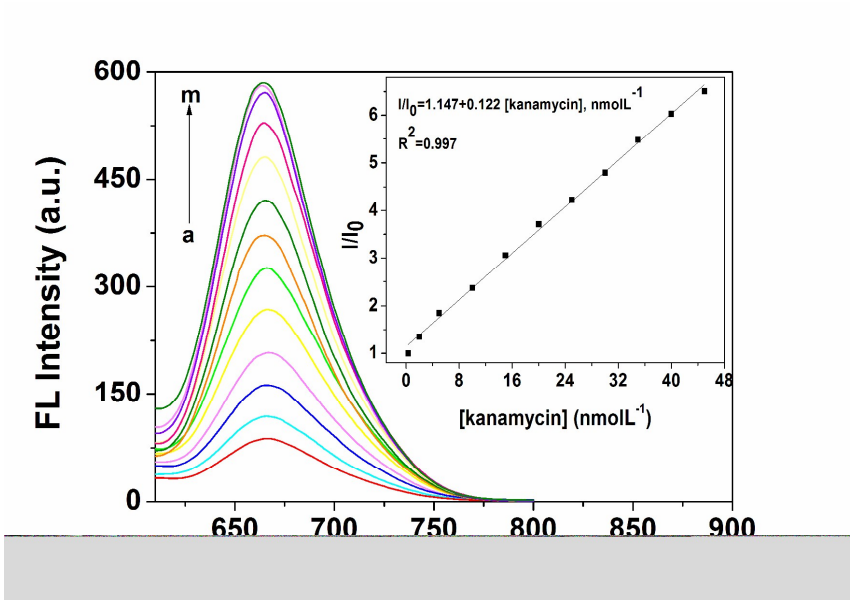

Fig. 6 The fluorescence spectra of Ky2-$CuInS_2$ QDs/GO in the presence of different concentrations of kanamycin in the range of 0-60 nmol·L^{-1} (a to m: 0, 0.3, 2.5, 5, 10, 15, 20, 25, 30, 35, 40, 45, 50 and 60 nmol·L^{-1}, respectively); Inset: The relationship between I/I_0 and the concentration of kanamycin in the range of 0.3-45 nmol·L^{-1}. I and I_0 were the fluorescence intensity of Ky2-$CuInS_2$ QDs/GO in the presence and absence of kanamycin, respectively. The mole ratio of aptamer to QDs was 1:544. The concentration of GO was 18.80 μg·mL^{-1}. The excitation wavelength was 590 nm.

Fig. 6 was the fluorescence spectra of Ky2-$CuInS_2$ QDs/GO system in the presence of different concentrations of kanamycin in the range of 0-60 nmol·L^{-1}. Fig. 6 inset was the relationship between I/I_0 (I and I_0 were the fluorescence intensity of Ky2-$CuInS_2$ QDs/GO in the presence and absence of kanamycin, respectively) and the concentration of kanamycin in the range of 0.3-45 nmol·L^{-1} (0.174-26.1 μg·L^{-1}). We can observe that the fluorescence intensity of Ky2-$CuInS_2$ QDs/GO system in the absence of kanamycin was quite weak. After adding kanamycin to the system, the

fluorescence intensity of the system gradually increased with the increasing concentration of kanamycin. There was good linearity between the fluoresence intensity ratio I/I_0 and the concentration of kanamycin in the range of 0.3-45 nmol·L^{-1} (0.174-26.1 μg·L^{-1}). The regression equation is I/I_0=1.147+0.122 [kanamycin], nmol·L^{-1}. The detection limit is 0.12 nmol·L^{-1} (0.070 μg·L^{-1}). The square of the corresponding regression coefficient (R^2) is 0.997. The detection limit is defined by the equation LOD=3σ/s, where σ is the standard deviation of the blank signals and s is the slope of the calibration curve. Fig. 7 was the fluorescence spectra of Ky2-$CuInS_2$ QDs in the presence of different concentrations of kanamycin in the range of 0-60 nmol·L^{-1}. It can be seen that the fluorescence intensity of Ky2-$CuInS_2$ QDs was not influenced by the addition of kanamycin in the concentration range from 0 to 60 nmol·L^{-1}, which indicated the interaction between kanamycin and Ky2-$CuInS_2$ QDs could be ignored.

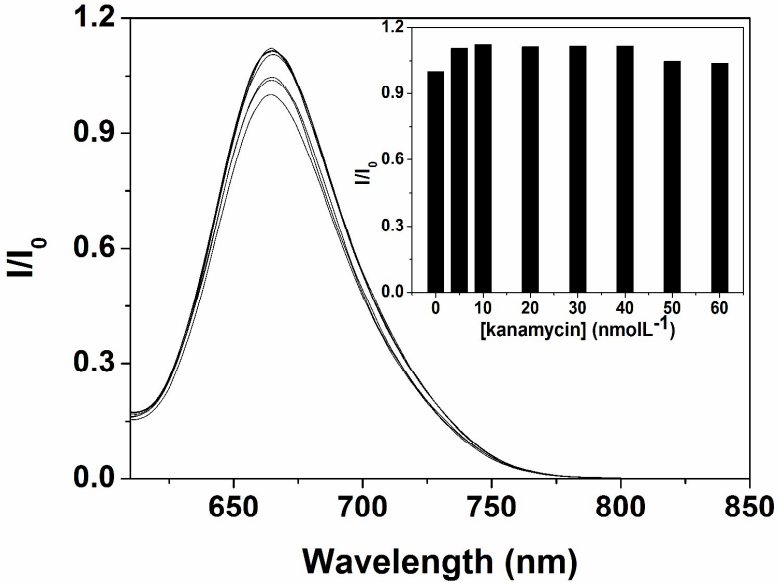

Fig. 7 The fluorescence spectra of Ky2-$CuInS_2$ QDs in the presence of different concentrations of kanamycin in

the range of 0-60 nmol·L^{-1} (bottom to up: 0, 5, 10, 20, 30, 40, 50 and 60 nmol·L^{-1}, respectively); Inset: The relationship between I/I_0 and the concentration of kanamycin. I and I_0 were the fluorescence intensity of Ky2-$CuInS_2$ QDs with and without of kanamycin, respectively. The mole ratio of aptamer to QDs was 1:544. The excitation wavelength was 590 nm.

3.4. Interference study

As we know, selectivity is a very important parameter to evaluate the performance of a new sensor, especially for one with potential applications in biosamples, a highly selective response to the target analyte over other potentially competing species is necessary. Thereby the selectivity of our nanosensor was further evaluated with various coexistence substances added. Table 1 showed the interference influence of some common inorganic ions and some analogous antibiotics including streptomycin, chloramphenicol, erythromycin, sulfadimethoxine and chlorotetracycline on the determination of kanamycin, a relative error of ±5.0% was considered to be tolerable. Tolerable concentration was defined as the concentrations of coexisting substances causing less than ±5.0% relative error. As found in Table 1, the tolerable concentration ratios of coexisting substances to 1 nmol·L^{-1} kanamycin was over 1000 fold for KCl, $MgCl_2$ and chlorotetracycline, 100 fold for streptomycin, chloramphenicol, erythromycin and sulfadimethoxine. Though GO could capture tetracycline antibiotics,[29] chlorotetracycline showed no obvious influence on the sensing ability of the present sensor. This was due to the adsorption of tetracycline onto graphene oxide exhibited a strong pH dependence. According to the previous reports, the adsorption

capacities decreased with the pH increasing, and acid medium facilitated the adsorption capacities. The other coexisting substances also showed little interference. Thus, the present method was suitable for selective detection of kanamyicn.

Table 1 The interference of coexisting substances on the detection of kanamycin (1 nmol·L^{-1})

Coexisting substance	Tolerable concentration	Molar ratio	ΔI/I (%)
K^+	1 mmol·L^{-1}	1000	1.92
Mg^{2+}	1 mmol·L^{-1}	1000	1.08
Na^+	1 mmol·L^{-1}	1000	0.95
Cl^-	1 mmol·L^{-1}	1000	1.23
glucose	1 mmol·L^{-1}	1000	2.59
streptomycin,	100 nmol·L^{-1}	100	2.34
chloramphenicol,	100 nmol·L^{-1}	100	1.37
erythromycin,	100 nmol·L^{-1}	100	1.42
sulfadimethoxine and	100 nmol·L^{-1}	100	1.06
chlorotetracycline	200 nmol·L^{-1}	200	3.80

ΔI = I_0-I, where I_0 and I are the fluorescence intensities of the Ky2-$CuInS_2$ QDs/GO/kanamycin system in absence and presence of interfering species. The mole ratio of aptamer to QDs was 1:544. The concentration of GO was 18.80 μg·mL^{-1}.

3.5. Detection of kanamycin in real samples

In order to evaluate the accuracy, repeatability and the practical application of the

present method, we determined kanamycin in the human serum, urine and milk samples and the results were listed in Table 2. The kanamycin content in the samples was derived from the standard curve and the regression equation. The average recovery test was made by using the standard addition method and the RSD was generally obtained from a series of three samples. It can be observed from Table 2 that that the RSD was lower than 3.0% and the average recoveries of kanamycin in the real samples were in the range of 96-103%, which indicated that the accuracy and precision of our sensing system were satisfactory. A comparison between this method and other reported methods for kanamycin detection in detection limit and linear range was summed up in Table S1. From Table S1, it could be found that the sensitivity of the present method was better than most of the reported methods.

Table 2 Results of kanamycin determination in the human serum, urine and milk samples

Sample	Original Found ($nmol \cdot L^{-1}$)	Added ($nmol \cdot L^{-1}$)	Total found ($nmol \cdot L^{-1}$)	Recovery (%)	RSD (n=3, %)
Serum	0.00	0.50	0.51	102	0.99
	0.00	1.00	0.99	99	2.35
	0.00	1.50	147	98	1.80
Urine	0.00	0.50	0.48	96	2.20
	0.00	1.00	0.97	97	1.04
	0.00	1.50	1.51	100.6	1.90
Milk	0.00	0.50	0.49	98	1.96
	0.00	1.00	1.04	100.4	2.91
	0.00	1.50	1.54	102.6	1.02

4. Conclusions

In summary, we have reported a simple, high sensitivity and selectivity nanosensor for

kanamycin detection by taking advantage of the fluorescence "turn-off" and "turn-on" feature of Ky2-$CuInS_2$ QDs. Under the optimum condition, a good linear response for kanamycin was found in the range of 0.3-45 nmol·L^{-1} (0.174-26.1 μg·L^{-1}), with a low detection limit of 0.12 nmol·L^{-1} (0.070 μg·L^{-1}), which is far below the MRL set by the European Union. The presented method was applied to detect kanamycin in the human serum, urine and milk samples with satisfactory results. Moreover, the current biosensing platform can offer a general approach for the detection of a range of biomedical and environmentally-relevant small molecules.

Acknowledgements

This work was financially supported by the Graduate Innovation Fund of Jilin University (No. 2015042), the National Natural Science Foundation of China (Nos. 21075050 and 21275063), the Science and Technology Development project of Jilin province, China (No. 20150204010GX) and the Open Founds of the State Key Laboratory of Electroanalytical Chemistry (SKLEAC201401).

1 **References**

1 D. Fourmy, S. Yoshizawa, J. D. Puglisi, *J. Mol. Biol.*, 1998, **277**, 333-345.

2 P. A. Bunn, *Med. Clin. N. Amer.*, 1970, **54**, 1245-1256.

3 R. Oertel, V. Neumeister, W. Kirch, *J. Chromatogr. A.*, 2004, **1058**, 197-201.

4 European Agency for the Evaluation of Medical Products (EMEA) London: 2003. Regulation No. EMEA/MRL/886/03-FINAL.

5 B. Blanchaert, E. P. Jorge, P. Jankovics, E. Adams, A. Van Schepdael, *Chromatographia*, 2013, **76**, 1505-1512.

6 W. Haasnoot, G. Cazemier, M. Koets, A. V. Amerongen, *Anal. Chim. Acta.*, 2003, **488**, 53-60.

7 E. Kaale, A. V. Schepdael, E. Roets, J. Hoogmartens, *Electrophoresis*, 2003, **24**, 1119-1125.

8 S. J. Yu, Q. Wei, B. Du, D. Wu, H. Li, L. G. Yan, H. M. Ma, Y. Zhang, *Biosensors and Bioelectronics*, 2013, **48**, 224-229.

9 S. R. Raz, M. G. E. G. Bremer, W. Haasnoot, W. Norde, Anal. Chem., 2009, **81**, 7743-7749.

10 J. J. Hill and C. A. Royer, *Methods Enzymol.*, 1997, **278**,390-416.

11 J. Zhang, J. Lei, C. Xu, L. Ding, H. Ju, *Analytical Chemistry*, 2010, **82**, 1117-1122.

12 A. Ansari, A. Kaushik, P. Solanki, B. Malhotra, *Electrochemistry Communications*, 2008, **10**, 1246-1249.

13 (a) M. Lan, C. Chen, Q. Zhou, Y. Teng, H. Zhao, X. Niu, *Advanced Materials Letters*, 2010, **1**, 217-224. (b) M. Yang, H. Li, A. Javadi, S. Gong, *Biomaterials*, 2010, **31**, 3281-3286.

14 (a) H. Mattoussi, J. M. Mauro, E. R. Goldman, G. P. Anderson, V. C. Sundar, F. V.

Mikulec and M. G. Bawendi, *J. Am. Chem. Soc.*, 2000, **122**, 12142-12150. (b) J. K. Jaiswal and S. M. Simon, *Trends Cell Biol.*, 2004, **14**, 497-504. (c) D. Zhou, M. Lin, Z. L. Chen, H. Z. Sun, H. Zhang, H. C. Sun, and B. Yang. *Chem. Mater.* 2011, **23**, 4857-4862.

15 S. J. Cho, D. Maysinger, M. Jain, B. Roder, S. Hackbarth, F. M. Winnik, *Langmuir*, 2007, **23**, 1974-1980.

16 (a) R. G. Xie, M. Rutherford, X. G. Peng, *J. Am. Chem. Soc.*, 2009, **131**, 5691-5697. (b) H. Nakamura, W. Kato, M. Uehara, K. Nose, T. Omata, S. O. Y. Matsuo, M. Miyazaki, H. Maeda, *Chem. Mater.*, 2006, 18, 3330-3335.

17 (a) F. Schedin, A. K. Geim, S. V. Morozov, E. W. Hill, P. Blake, M. I. Katsnelson and K. S. Novoselov, *Nat. Mater.*, 2007, **6**, 652-655. (b) F. Barroso-Bujans, S. Cerveny, R. Verdejo, J. J. del Val, J. M. Alberdi, A. Alegria and J. Colmenero, *Carbon*, 2010, **48**, 1079-1087.

18 (a) C. H. Lu, H. H. Yang, C. L. Zhu, X. Chen, G. N. Chen, *Angew. Chem. Int. Ed.*, 2009, **48**, 4785-4787. (b) X. Q. Liu, R. Aizen, R. Freeman, O. Yehezkeli, I. Willner, *ACS nano*, 2012, **6**, 3553-3563.

19 (a) H. X. Chang, L.H. Tang, Y. Wang, J.H. Jiang, J.H. Li, *Anal. Chem.*, 2010, **82**, 2341-2346. (b) Q. S. Chen, W. L. Wei, J. M. Lin, *Biosens. Bioelectron.*, 2011, **26**, 4497-4502.

20 M. Zhang, B.C. Yin, X.F. Wang, B.C. Ye, *Chem. Commun.*, 2011, **47**, 2399-2401.

21 C. L. Zhang, Y. X. Yuan, S. M. Zhang, Y. H. Wang, Z. H. Liu, *Angew. Chem. Int. Ed.*, 2011, **50**, 6851-6854.

22 C. H. Lu, H. H. Yang, C. L. Zhu, X. Chen, G. N. Chen, *Angew. Chem. Int. Ed.*, 2009, **48**, 4785-4787.

23 Y. P. Xing, C. Liu, X. H. Zhou, H. C. Shi, *Scientific Reports*, 2015. DOI:

10.1038/srep08125.

24 A. D. Keefe, S. Pai, A. Ellington, *Nat. Rev. Drug Discov.*, 2010, **9**, 537-550.

25 F. Ortmann, W. G. Schmidt, F. Bechstedt, *Phys. Rev. Lett.*, 2005, **95**, 186101 (1-4).

26 S. J. He, B. Song, D. Li, C. F. Zhu, W. P. Qi, Y. Q. Wen, L. H. Wang, S. P. Song, H. P. Fang and C. H. Fan, *Adv. Funct. Mater.*, 2010, **20**, 453-459.

27 Y. W. Zhu, S. Murali, W. W. Cai, X. S. Li, J. W. Suk, J. R. Potts, R. S. Ruoff, *Adv. Mater.*, 2010, **22**, 3906-3924.

28 S. Y. Liu, H. Zhang, Y. Qiao and X. G. Su, *RSC Advances*, 2012, **2**, 819-825.

29 Y. Gao, Y. Li, L. Zhang, H. Huang, J. J. Hu, S. M. Shah, X. G. Su, *J. Colloid Interface Sci.*, 2012, **368**, 540-546.

30 R. Xie, M. Rutherford and X. Peng, *J. Am. Chem. Soc.*, 2009, **131**(15), 5691-5697.

31 Z. P. Liu, G. Y. Li, Q. Ma, L. L. Liu, X. G. Su, Microchim Acta, 2014, **181**, 1385-1391.

32 T. C. Prathna, N. Chandrasekaran and A. Mukherjee, *Colloids Surf.*, A, 2011, **390**, 216-224.

33 Z. P. Liu, Z. H. Lin, L. L. Liu, X. G. Su, *Analytica Chimica Acta*, 2015, **876**, 83-90.

34 H. Li, D. E. Sun, Y. J. Liu, Z. H. Liu, *Biosensors and Bioelectronics*, 2014, **55**, 149-156.

35 A. Hoshino, K. Fujioka, T. Oku, M. Suga, Y.F. Sasaki, T. Ohta, M. Yasuhara, K. Suzuki, K. Yamamoto, *Nano Letters*, 2004, 4, 2163-2169.

36 L.M. Qi, H. Cölfen, M. Antonietti, *Nano Letters*, 2001, 1, 61-65.

37 K. H. Leung, H. Z. He, D. S. H. Chan, W. C. Fu, C. H. leung, D. L. Ma, *Sens. Actuators B.*, 2013, **177**, 487-492.

38 K. M. Song, M. Cho, H. Jo, K. Min, S. H. Jeon, T. Kim, M. S. Han, J. K. Ku and

C. Ban, *Anal. Biochem.*, 2011, **415**, 175-181.

39 X. Sun, F. L. Li, G. H. Shen, J. D. Huang, X. Y. Wang, *Analyst*, 2014, **139**, 299-308.

A novel aptamer-mediated fluorescence "turn off-on" nanosensor for highly sensitive and selective detection of kanamycin using $CuInS_2$ quantum dots@graphene oxide